International Journal of Advanced Engineering, Management and Science (IJAEMS)
Peer-Reviewed Journal
ISSN: 2454-1311 | Vol-12, Issue-6; Nov-Dec, 2026
Journal Home Page: https://ijaems.com/
DOI: https://dx.doi.org/10.22161/ijaems.126.3

ROS-Based Design and Gait Cooperative Control of a Tennis-Collecting Quadruped Robot

Hung-Yu Chen[1], Yi-Pin Ko[2], Ho-Sheng Chen[3*]

[1]Guangzhou Institute of Science and Technology, China
Email:ronwisely@outlook.com
[2]iSensetek technology., Inc
Email:ak@isensetek.com
[3]School of Sciences, Guangdong University of Petrochem Technology (GDUPT), Maoming 525000, China
[*]Corresponding author:Ho-Sheng Chen
Email: hschen98.tw@gmail.com

Received: 19 Oct 2026; Received in revised form: 14 Nov 2026; Accepted: 19 Nov 2026; Available online: 26 Nov 2026

Abstract**—***Quadruped robot platforms can help people finish routine work and carry out patrols in dangerous areas that humans cannot easily reach. Boston Dynamics Spot is a well known overseas product, capable of precise movement, object identification and emergency handling. It has been used for rescue, home service and object transportation. China is also making progress in developing its own quadruped robots for civilian and military uses. However, most existing quadruped robots come with high development costs. Targeting the practical need of collecting tennis balls, this paper develops a small quadruped robot with basic movement and ball collection functions. The system uses Raspberry Pi as the main control board. Peripheral hardware includes a six axis sensor IC for acceleration and attitude detection, a buzzer, PWM servo interfaces, operation buttons, power indicator, voltage display port, fan port, charging port and power port. This work offers a practical low cost hardware reference for small service oriented quadruped robots.*

Keywords**— quadruped robot, Raspberry Pi, six-axis sensor, PWM servo, tennis-ball collection**

I. INTRODUCTION

Robotic technology has gained rapid progress driven by advanced control chips, integrated circuits and new mechanical materials[1]. A wide range of robotic devices are now applied in industrial production and daily service scenarios. Artificial intelligence and mechatronics further promote the upgrading of traditional industries[2]. Automated production lines reduce manual work in automobile manufacturing, and various robot prototypes have been displayed at robot exhibitions. Machine-learning-based AI technologies have also shown practical value in many fields[3].

Conventional wheeled or tracked robots cannot move well in forests, wetlands and hilly terrains[4]. Quadruped bionic robots possess better terrain adaptability for these unstructured environments. Compared with biped and hexapod robots, they reach a reasonable trade-off between mechanical complexity and motion stability[5]. Considering the growing demand for service-type bionic robots, this paper carries out research on a quadruped robot for tennis-ball collection. The main contents include machine-vision perception, gait adjustment and the design of ball-collecting mechanism[6].

Domestic research institutions and enterprises have invested much effort in quadruped robot development over recent years. However, bottlenecks still exist in core components and control algorithms[7]. Since the 1980s, Chinese universities have conducted systematic research on quadruped locomotion. Some representative prototypes have been developed with government project support, and commercial products such as Unitree G01 also achieve competitive performance. Overseas exploration of legged robots started earlier. Researchers have put forward key gait parameters and stability evaluation criteria[8]. Technologies including CPG-based control and dynamic decoupled control were proposed to realize trot, pace and other typical gaits. Advanced platforms such as ANYmal and Boston Dynamics Spot demonstrate outstanding

©2026 The Author(s). Published by Infogain Publication, This work is licensed under a Creative Commons Attribution 4.0 License. http://creativecommons.org/licenses/by/4.0/

dynamic performance[9]. Meanwhile, open-source frameworks represented by ROS greatly lower the development threshold for university research projects[10].

Nevertheless, most commercially available quadruped robot platforms are costly. There are relatively few low-cost prototypes targeting simple on-site object-collection tasks. Against this background, this paper designs a ROS-based quadruped robot for tennis-ball collection. Hardware component selection, kinematic analysis, gait planning, OpenCV-supported visual recognition and ball-collecting mechanism are described in detail. Both simulation and prototype experiments are performed to verify the overall system performance.

II. HARDWARE CIRCUIT DESIGN AND COMPONENT SELECTION

A quadruped robot must reconcile real-time computation, multi-joint actuation, attitude sensing and visual input within a tight volume and power budget. This chapter follows a layered "compute core–interface expansion–actuator–perception–end–effector" sequence for component selection, and adopts modular integration to reduce wiring complexity and commissioning risk.

The compute core is a Raspberry Pi 4 Model B. Compared with its predecessors in Fig. 1, it features a quad-core Cortex-A72 processor, Gigabit Ethernet, dual-band 802.11ac Wi-Fi and Bluetooth 5.0; its USB 3.0 port can directly host a high-definition camera stream, meeting the concurrency requirement of visual inference and synchronized multi-servo scheduling. The abundant GPIOs and the mature open-source stack (Linux + ROS + OpenCV) lower the deployment barrier, making it suitable as an upper controller for research and teaching quadrupeds.

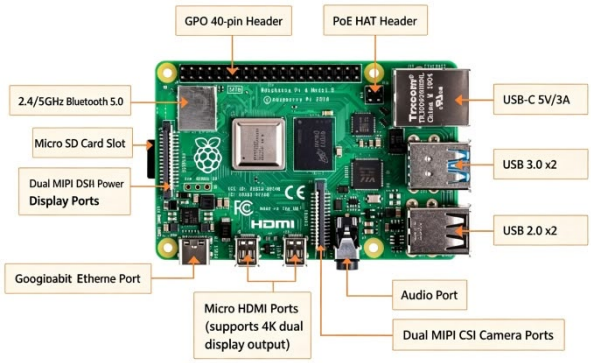

Fig. 1 ： Raspberry Pi 4B board and interface layout.

Fig. 2 shows the board. Stacked on the 40-pin header, the carrier replaces point-to-point jumpers with board-level connectors for servos, power and sensors, which lowers the overall height and separates power and signal traces for better EMC and maintainability.

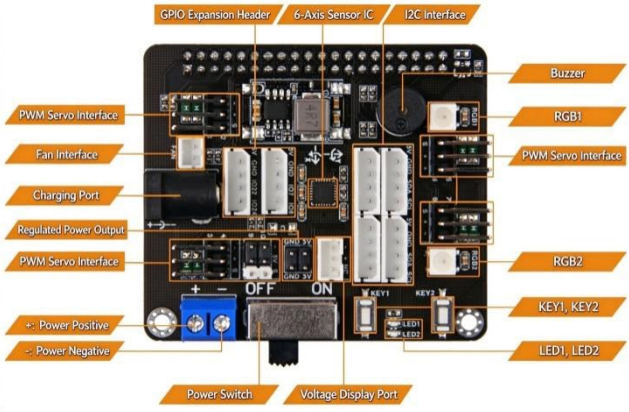

Fig. 2 ： Raspberry Pi 4B board and interface layout.

Quadruped locomotion demands actuators that are light yet torque-dense and responsive. The HPS-0618SG coreless-DC servo is selected. Eight units are used—four for the hip joints and four for the knees—driven by PWM pulses and connected directly to the carrier's servo bus *in Table 1*.

Table 1 ：Actuator: Coreless-DC Servo Parameters

Parameters	Values	Implication
Operating voltage	8.4 V	Matches Li-ion supply
Stall torque	≥ 8 kg·cm	Static load capacity
No-load speed	≤ 0.06 s/60°	Swing-phase timing
Range	0°–180°	Workspace coverage
Motor	Coreless	Low inertia & high efficiency
Gear	Stainless steel	Impact-resistant
Control	PWM pulse	No extra driver IC

The coreless rotor removes the iron core, eliminating iron loss and cogging torque; it therefore offers higher power-conversion efficiency, lower rotor inertia and faster start–stop response, and fatigues less under the frequent reversal of gait cycles than a conventional brushed servo. Note, however, that 8 kg·cm is the usable upper bound for a small servo: the gait planner should avoid holding the hip at maximum moment arm and keep the center of mass inside the stability region through the x_shift balance parameter.

©2026 The Author(s). Published by Infogain Publication, This work is licensed under a Creative Commons Attribution 4.0 License. http://creativecommons.org/licenses/by/4.0/

The input quality of the vision subsystem sets the upper bound of subsequent color segmentation and target localization. The Pi 4B's USB 3.0 port is compatible with most UVC cameras; to leave room for 3-D environment perception and obstacle avoidance, depth/stereo capability is prioritized among the candidates in Table 2.

Table 2 ： Candidate

Candidate	Type	Fit to this work
Intel RealSense D435	Active IR depth	High indoor accuracy; heavier on compute
Orbbec Astra Pro	Structured-light depth	Plug-and-play; good for mapping
ZED Stereo Camera	Stereo rig	Requires stereo calibration
Asus Xtion Pro Live	Depth camera	Point-cloud output for scene understanding

Balancing size, driver maturity and the Pi-side compute budget, a standard USB color camera running at 640×480 is used in the algorithm-validation stage, with color plus contour used for ball detection. The depth camera is reserved as an upgrade interface, so that the 2-D pixel offset can later be converted to a metric range and improve approach accuracy.

The frame must stay stiff under locomotion impacts and collection reaction forces while keeping inertia low. The body consists of three printed assemblies—main shell, thigh and shank—mated with metal servo horns; each leg is a two-link mechanism driven by one hip servo and one knee servo. Fig. 3 shows the 3-D model: the four legs are symmetrically placed at the corners, with the center of mass projected near the middle of the support polygon.

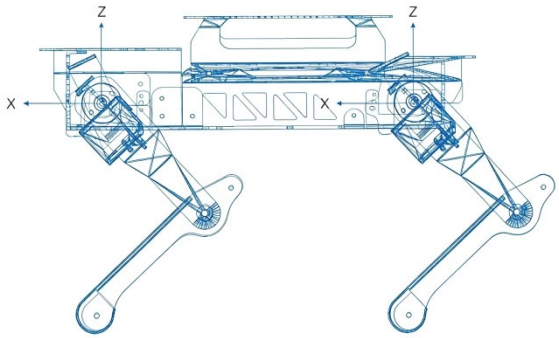

Fig. 3 ： 3-D model and leg configuration of the robot.

The end-effector is what distinguishes this project from a general-purpose quadruped. Three concepts were evaluated during prototyping; the iteration itself forms the mechanism-design trajectory. Fig. 4 shows the first two roller-based versions.

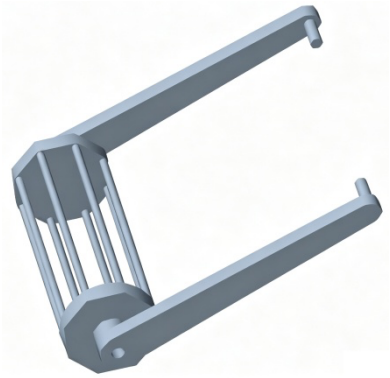

Fig. 4 ： Two iterative versions of the roller collector.

Concept A: elastic roller. The ball is squeezed into the hopper by compliant rods—simple, but locomotion vibration tends to bounce the ball away; a light body cannot override the elastic rebound by weight.

Concept B: dorsal gripper. Grasps the ball after localization, but needs extra servos and degrees of freedom, exceeding the prototype schedule.

Concept C (adopted): biomimetic kicking. Reuses the swing phase of a leg to kick the ball into a front hopper—no extra actuator, and it shares the gait controller by design.

The final scheme treats collection as a controlled kick: vision supplies the lateral offset, the gait controller fine-tunes the stance, then a foreleg executes a short swing and the ball rolls into the hopper. This reduces the end-effector from "an added gripper" to "hopper plus gait strategy," cutting both mass and failure points.

The quadruped robot system for tennis ball collection is described below Fig. 5. This design adopts a roller-type structure.

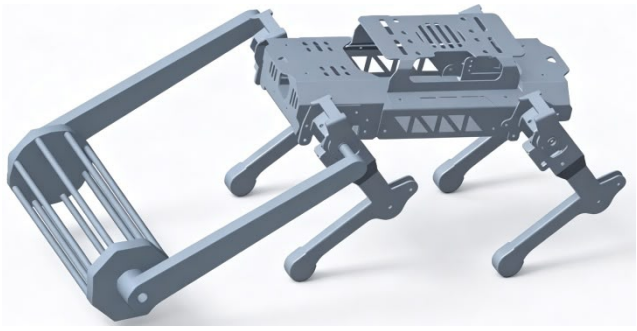

Fig. 5 ： Schematic diagram of the quadruped robot system for tennis ball collection.

©2026 The Author(s). Published by Infogain Publication, This work is licensed under a Creative Commons Attribution 4.0 License. http://creativecommons.org/licenses/by/4.0/

III. SYSTEM DESIGN AND GAIT COOPERATIVE CONTROL

The robot is organized as a three-layer perception, decision, and execution loop as Fig. 6. The perception layer comprises a USB camera and an on-board 6-axis IMU, supplying target imagery and body attitude. The decision layer, running on the Pi 4B, performs color segmentation, target localization and gait-phase scheduling. The execution layer drives eight PWM channels through the carrier to the hip and knee servos for walking and kicking.

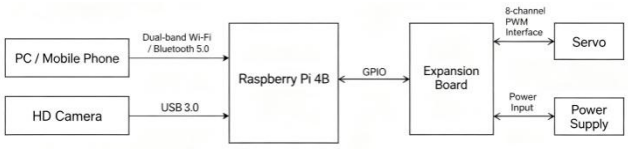

Fig. 6 : Overall system architecture of the tennis-collecting robot

The design goal is decomposed into six verifiable requirements: (1) stable gait with correct phasing; (2) real-time read-back of attitude and tuning parameters over wireless link (Wi-Fi/LAN or VNC direct); (3) on-board target recognition and stance decision; (4) logging of parameters and run traces to the SD card; (5) basic adaptation to illumination and background variation; and (6) automatic halt with an error code reported on target loss or attitude violation. These six items serve as the commissioning and acceptance criteria.

Fig. 7 shows the electrical interconnection: the carrier stacks on the Pi's 40-pin header; the eight servos and the collector interface are powered and governed by the on-board servo bus, while the camera connects directly to the USB 3.0 port. The control path are Pi, carrier, and servos/collector, and the sensing path are camera, USB, Pi, and OpenCV solver. This hierarchical, one-way chained topology decouples vision from joint control and simplifies module-level debugging.

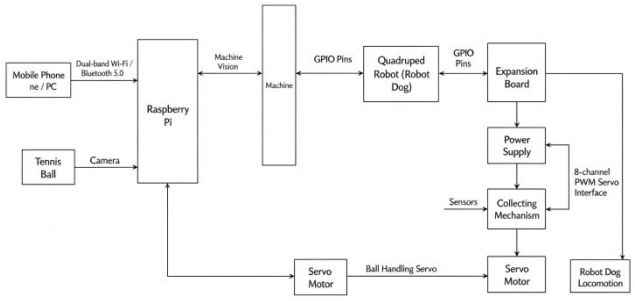

Fig. 7 : Hardware interconnection block diagram.

A fixed frame must be defined before gait solving. The origin O is placed at the geometric center of the four hip centers, with X forward, Z downward and Y completing the right-handed set. Because each leg is driven in the sagittal plane by only two servos (hip and knee), the foot is specified by X and Z only and the Y command is ignored by the inverse solver. Coordinates are in centimeters. At the standing pose all four feet are (0, 0, −10), where |Z| = 10 cm is the vertical leg length below the origin and X = 0 means the hip–foot line is vertical in the sagittal plane. A 2-cm forward body shift is realized simply by setting the foot target to X = 2; the inverse kinematics then returns a new joint angle set. This is the essence of "foot-trajectory-driven locomotion."

Each leg is abstracted as a planar two-link chain: thigh length l_1, shank length l_2, hip angle θ_1 from the body-mounted servo, knee angle θ_2 from the leg-mounted servo, and foot coordinate (x, y) (here y is the in-plane longitudinal coordinate, i.e. the Z component in the body frame). Fig. 8 defines the joints and links.

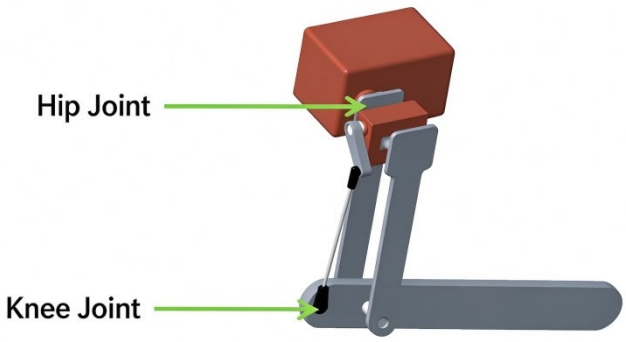

Fig. 8 : Two-link leg: joint and link definition.

According to the forward kinematics analysis, the solving steps are as follows: by utilizing the servo rotation angles, the ultimate end-effector position of the robot can be calculated as Fig. 9.

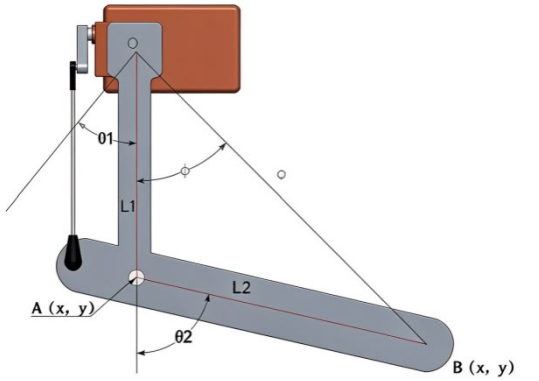

Fig. 9 : Establishment of the Forward Kinematics Coordinate System.

First, based on the coordinate expression of A(x, y)

$$x = l_1 \cos\theta_1 \quad (1)$$

©2026 The Author(s). Published by Infogain Publication, This work is licensed under a Creative Commons Attribution 4.0 License. http://creativecommons.org/licenses/by/4.0/

$$y = I_1 \sin\theta_1 \quad (2)$$

Next, B(x', y') is expressed by applying the rotation transformation.

$$x' = l_2 \cos\theta_1 \cos\theta_2 - l_2 \sin\theta_1 \sin\theta_2 + x \quad (3)$$

$$y' = l_2 \sin\theta_1 \cos\theta_2 + l_2 \cos\theta_1 \sin\theta_2 + y \quad (4)$$

Based on the inverse kinematics analysis, the solving process is as follows: First, according to the foot-end coordinates, the kinematic positions of the knee and hip joints are calculated to further solve for the corresponding servo rotation angles. Then, based on these servo rotation angles, the corresponding control values are calculated to directly drive the servos, thereby achieving the control of the robot. Taking O as the origin and aa as the common side, according to the foot-end coordinates (x,y), we have: $a^2=x^2+y^2$. Based on the Pythagorean theorem, as shown in Fig. 10.

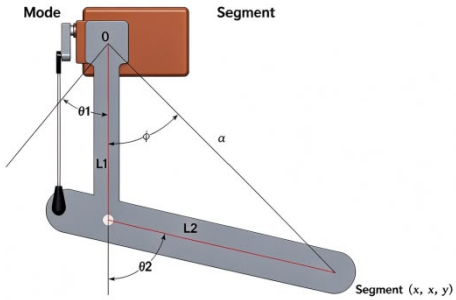

Fig. 10 : Establishment of the Inverse Kinematics Coordinate System

$$a^2 = I_1^2 + I_2^2 - 2I_1I_2\cos(180^\circ - \theta_2) \quad (5)$$

Then, we have:

$$X^2 + Y^2 = I_1^2 + I_2^2 - 2I_1I_2\cos(180^\circ - \theta_2) \quad (6)$$

By rearranging the terms, we obtain:

$$\cos(180^\circ - \theta_2) = \frac{-(I_1^2 + I_2^2 - X^2 - Y^2)}{-2I_1I_2} \quad (7)$$

$$\cos(180^\circ - \theta_2) = \frac{X^2 + Y^2 - I_1^2 - I_2^2}{-2I_1I_2} \quad (8)$$

$$180^\circ - \theta_2 = arc\cos(\frac{X^2 + Y^2 - I_1^2 - I_2^2}{-2I_1I_2}) \quad (9)$$

$$\theta_2 = 180^\circ - arc\cos(\frac{X^2 + Y^2 - I_1^2 - I_2^2}{-2I_1I_2}) \quad (10)$$

The D-H analysis aims to describe the displacement and rotation relationships between adjacent links. Denavit and Hartenberg introduced a systematic matrix method for establishing coordinate systems for each successive link. In the D-H notation, a 4×4 matrix is used to represent the coordinate transformation from one joint to the previous joint. Consequently, through successive transformations, the initial coordinates can be mapped to the base coordinates. For the DH analysis of the robot's leg, the DH coordinate system is first established. Based on the right-hand rule, the base coordinate system is defined by Z_0, X_0, and Y_0, as illustrated in Fig. 11.

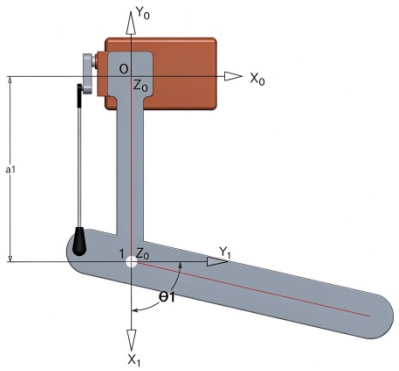

Fig. 11 : Establishment of the D-H Coordinate System

Explanation of D-H parameters:

θ_1: The rotation angle from the X_0 axis to the X_1 axis about the Z_0 axis, determined by the right-hand rule.

d_1: The distance from the origin of the 0th coordinate system to the intersection of the X_1 and Z_0 axes; in this case, $d_1=0$.

a_1: The shortest distance between the Z_0 and Z_1 axes.

α_1: The rotation angle from the Z_0 axis to the Z_1 axis about the X_1 axis, determined by the right-hand rule; in this case, $\alpha_1=0$.

From the D-H coordinate diagram, it can be observed that the 0th coordinate frame is transformed to the 1st coordinate frame through rotation and translation. The specific steps are as follows:

The 0th coordinate system is translated along the Z_0 axis by a distance d_1 to align the origins of the 0th and 1st coordinate systems. The corresponding transformation matrix is as follows:

$$T(z,d) = \begin{bmatrix} 1 & 0 & 0 & 0 \\ 0 & 1 & 0 & 0 \\ 0 & 0 & 1 & d_i \\ 0 & 0 & 0 & 1 \end{bmatrix} \quad (11)$$

By rotating the 0th coordinate system about the Z_0 axis, the X_0 axis is aligned to be collinear with the X_1 axis. The transformation matrix is expressed as:

$$T(z,\theta) = \begin{bmatrix} c\theta_1 & -s\theta_1 & 0 & 0 \\ s\theta_1 & c\theta_1 & 0 & 0 \\ 0 & 0 & 1 & 0 \\ 0 & 0 & 0 & 1 \end{bmatrix} \quad (12)$$

By translating the 0th coordinate system along the X_1 axis by a distance a_1, it coincides with the 1st coordinate system. The transformation matrix is expressed as:

©2026 The Author(s). Published by Infogain Publication, This work is licensed under a Creative Commons Attribution 4.0 License. http://creativecommons.org/licenses/by/4.0/

$$T(z,a)=\begin{bmatrix}1&0&0&a_1\\0&1&0&0\\0&0&1&0\\0&0&0&1\end{bmatrix} \quad (13)$$

By rotating the 0th coordinate system about the X_1 axis by an angle α_1, the two coordinate systems are aligned to coincide. The transformation matrix is expressed as:

$$T(z,\alpha)=\begin{bmatrix}0&0&0&0\\0&c\alpha_1&-s\alpha_1&0\\0&s\alpha_1&c\alpha_1&0\\0&0&0&1\end{bmatrix} \quad (14)$$

Consequently, the resulting transformation matrix ${}^0A_1$ can be calculated by multiplying the four transformation matrices mentioned above.

$${}^0A_1 = T(z,d)\,T(z,\theta)\,T(z,a)\,T(z,\alpha) \quad (15)$$

Substituting the above expressions into the (15) gives:

$${}^0A_1=\begin{bmatrix}c\theta_1&-c\alpha_1c\theta_1&s\alpha_1c\theta_1&0\\s\theta_1&c\alpha_1c\theta_1&-s\alpha_1c\theta_1&0\\0&s\alpha_1&c\alpha_1&d_1\\0&0&0&1\end{bmatrix} \quad (16)$$

The inverse matrix is:

$${}^1A_0=({}^0A_1)=\begin{bmatrix}c\theta_1&s\theta_1&0&-a_1\\-c\alpha_1s\theta_1&c\alpha_1c\theta_1&s\alpha_1&-d_1s\alpha_1\\s\alpha_1s\theta_1&-s\alpha_1c\theta_1&0&-d_1c\alpha_1\\0&0&0&1\end{bmatrix} \quad (17)$$

Substituting $d_1=0$ and $\alpha_1=0$ into the equation yields:

$${}^1A_0=({}^0A_1)=\begin{bmatrix}c\theta_1&s\theta_1&0&-a_1\\s\theta_1&c\theta_1&0&0\\0&0&0&0\\0&0&0&1\end{bmatrix} \quad (18)$$

The D-H transformation matrix is obtained once the values of a_1 and θ_1 of the robot dog are confirmed.

IV. CONCLUSION

The tennis-ball collecting quadruped robot is developed based on the open-source ROS platform. Community resources greatly lower the development threshold for quadruped robot research. Gait control, which relies on inverse kinematics analysis, is a key difficulty in this design. Open-source gait modules help achieve stable robot locomotion. Machine vision using OpenCV is adopted to recognize tennis-ball targets and guide robot movement.

Open-source robotics and upper-computer tools make robot development more accessible for ordinary developers. Robots have shown great value in industry, service, medical treatment and agriculture. As core supporting technology, machine vision is booming in China with policy support.

Different from wheeled robots, quadruped robots realize complex motions such as running and stair-climbing through sensors and programming, showing good environmental adaptability. The prototype still needs further improvement. Future work will focus on visual anti-interference performance, gait stability with the collector and mechanical reliability of the ball-collecting structure.

ACKNOWLEDGEMENTS

This research was supported by “Guangdong Science and Technology Program”, “Research on Investigation of the Multimodal Intelligent Flying Electric Motorcycle's Autonomous Motion. (NO. 2024A0505050019)”.

REFERENCES

[1] Ulloa, C. C., Sánchez, L., Del Cerro, J., & Barrientos, A. (2023). Deep Learning Vision System for Quadruped Robot Gait Pattern Regulation. *Biomimetics*, 8(3), 289. http://dx.doi.org/10.3390/biomimetics8030289

[2] Kim, J., Park, J., & Kim, J. (2022). A Review of Recent Advancements in Quadruped Bionic Robot Systems. *Journal of Bionic Engineering*, 19(4), 721-742. http://dx.doi.org/10.1007/s42235-022-00198-5

[3] Zhang, H., Li, Y., & Wang, L. (2021). ROS-Integrated Hardware-Software Co-Simulation Framework for Small-Scale Quadruped Robots. *IEEE Access*, 9, 148762-148774. http://dx.doi.org/10.1109/ACCESS.2021.3124371

[4] Wu, T., & Liu, Y. (2022). OpenCV-Based Object Detection for Low-Cost Embedded Quadruped Robot Platform. *Sensors*, 22(17), 6428. http://dx.doi.org/10.3390/s22176428

[5] Focchi, M., Semini, C., & Boaventura, T. (2021). Dynamic Gait Planning for Quadruped Robots on Uneven Terrain: Review and Experimental Validation. *Robotics and Autonomous Systems*, 141, 103781. http://dx.doi.org/10.1016/j.robot.2021.103781

[6] Li, Z., Gao, F., & Yu, Z. (2023). Development Status and Technical Challenges of Domestic Quadruped Robots in China. *International Journal of Advanced Robotic Systems*, 20(2), 1-16. http://dx.doi.org/10.1177/17298806231162743

[7] Napinas, R., & Zhang, E. (2023). Playing Catch with Boston Dynamics’ Spot: Object-Detection-Based Interactive Task for Quadruped Robot. *Proceedings of the Student Conference on Robotics (SCR)*, pp.41-46. http://dx.doi.org/10.21223/P3K45S

[8] Sun, Y., Zhou, K., & Chen, W. (2024). Central Pattern Generator-Inspired Adaptive Gait Control for Small-Size Servo-Driven Quadruped Robot. *Applied Sciences*, 14(5), 2041. http://dx.doi.org/10.3390/app14052041

[9] Yang, C., Shi, G., & Xu, H. (2022). Review of Open-Source Software Stacks for Quadruped Robot Prototyping. *Journal of Robotics*, 2022, 1-14. http://dx.doi.org/10.1155/2022/9876542

[10] Lee, S., & Choi, J. (2025). Vision-Guided Object Retrieval Task Implementation for Low-Cost Quadruped Robot Prototype. *International Journal of Mechanical Engineering and Robotics Research*, 14(1), 89-97. http://dx.doi.org/10.18178/ijmerr.14.1.89-97

©2026 The Author(s). Published by Infogain Publication, This work is licensed under a Creative Commons Attribution 4.0 License. http://creativecommons.org/licenses/by/4.0/